Supporting Information

Reichenbach et al. 10.1073/pnas.0914345107

SI Text

Here we further describe our modeling approach. We provide a detailed description of the two-mass model for the organ of Corti and discuss the energy balance. We then turn to the hydrodynamics of the cochlea. Because our goal is to demonstrate a principle rather than to describe the cochlea in full detail, we focus on a basic, one-dimensional model. We conclude with a model for the regulation of the OHCs' membrane potential, which demonstrates how the critical mechanomotility coefficient α_* can result.

Micromechanics of the Organ of Corti. To describe the micromechanics of the organ of Corti we employ a model with two degrees of freedom: the motion of the basilar membrane and the motion of the hair-bundle complex (Fig. 2*B*). The impedance Z_{BM} of the basilar membrane results from a mass m_{BM}, viscous damping λ_{BM}, and stiffness K_{BM}. Similarly, the impedance of the complex formed by the hair bundles, reticular lamina, and tectorial membrane involves mass m_{TM}, viscous damping λ_{HB}, and stiffness K_{HB}.

The motions of the basilar membrane and of the hair-bundle complex are coupled through the impedance Z_{C} of the organ of Corti, which possesses viscous and elastic contributions λ_{C} and K_{C}. Further coupling arises through the combined OHCs and Deiters' cells (Fig. S1). An OHC can be described as a piezoelectric element (1). Its length change δL depends both on a change δV in the membrane potential as well as on the applied force F. Considering oscillatory motions at angular frequency $\omega = 2\pi f$ we can write $\delta L = \widetilde{\delta L} e^{i\omega t} + c.c.$, $\delta V = \widetilde{\delta V} e^{i\omega t} + c.c.$, and $F = \tilde{F} e^{i\omega t} + c.c.$ in which $c.c$ denotes the complex conjugate. The length change then follows as

$$\widetilde{\delta L} = -c\widetilde{\delta V} + c_2 \tilde{F} \qquad \text{[S1]}$$

with coefficients c, c_2. We define $\tilde{X}_{\mathrm{EE}} = -c\widetilde{\delta V}$ as the part of the length change that results from voltage changes alone. The length change $c_2\tilde{F}$ results from the OHC's viscoelasticity $Z_{\mathrm{OHC}} = -i\omega^{-1}c_2^{-1}$ in series with X_{EE} (Fig. S1). It lies in series with the Deiters' cell which can be described as another viscoleastic element Z_{DC}. The two viscoelastic elements Z_{OHC} and Z_{DC} in series combine into the viscoelastic element

$$Z_{\mathrm{D}} = (Z_{\mathrm{OHC}}^{-1} + Z_{\mathrm{DC}}^{-1})^{-1} \qquad \text{[S2]}$$

such that the schematic of Fig. 2B results. We denote by K_{D} the elastic component and by λ_{D} the viscous part of the impedance Z_{D}. The equations of motion for hair-bundle and basilar-membrane displacement, X_{HB} and X_{BM}, respectively, then read

$$\begin{aligned} &m_{\mathrm{TM}}\partial_t^2 X_{\mathrm{HB}} + \lambda_{\mathrm{HB}}\partial_t X_{\mathrm{HB}} + K_{\mathrm{HB}} X_{\mathrm{HB}} \\ &\quad + (K_D + \lambda_D\partial_t)(X_{\mathrm{HB}} - X_{\mathrm{EE}} - X_{\mathrm{BM}}) \\ &\quad + (K_C + \lambda_C\partial_t)(X_{\mathrm{HB}} - X_{\mathrm{BM}}) \\ &\quad = F_{\mathrm{int}}, \end{aligned} \qquad \text{[S3]}$$

$$\begin{aligned} &m_{\mathrm{BM}}\partial_t^2 X_{\mathrm{BM}} + \lambda_{\mathrm{BM}}\partial_t X_{\mathrm{BM}} + K_{\mathrm{BM}} X_{\mathrm{BM}} \\ &\quad - (K_D + \lambda_D\partial_t)(X_{\mathrm{HB}} - X_{\mathrm{EE}} - X_{\mathrm{BM}}) \\ &\quad - (K_C + \lambda_C\partial_t)(X_{\mathrm{HB}} - X_{\mathrm{BM}}) \\ &\quad = F_{\mathrm{ext}}. \end{aligned} \qquad \text{[S4]}$$

A sound stimulus at angular frequency ω provides an external force F_{ext} on the basilar membrane whose dependence on time t may be written as $F_{\mathrm{ext}}(t) = \tilde{F}_{\mathrm{ext}} e^{i\omega t} + c.c.$ with the Fourier coefficient $\tilde{F}_{\mathrm{ext}}$. The evoked oscillations of the basilar membrane, X_{BM}, and of the hair-bundle complex, X_{HB}, occur dominantly at the same frequency f; additional frequencies may arise from nonlinear effects owing to internal forces in the hair bundle. We consider the corresponding Fourier coefficients $\tilde{X}_{\mathrm{BM}}$ and $\tilde{X}_{\mathrm{HB}}$. The electrically evoked length change $\tilde{X}_{\mathrm{EE}}$ of OHCs depends linearly on the hair-bundle displacement, for the membrane-potential change depends linearly on hair-bundle motion (see Supplementary Section on the electrical regulation of the OHC membrane potential): $\tilde{X}_{\mathrm{EE}} = -\alpha\tilde{X}_{\mathrm{BM}}$ with a complex, frequency-dependent mechanomotility coefficient α. Eq. **S4** then yields Eqs. **1** and **2** with

$$Z_{\mathrm{HB}} = i\omega m_{\mathrm{TM}} + \lambda_{\mathrm{HB}} - i\omega^{-1}K_{\mathrm{HB}}, \qquad \text{[S5]}$$

$$Z_{\mathrm{BM}} = i\omega m_{\mathrm{BM}} + \lambda_{\mathrm{BM}} - i\omega^{-1}K_{\mathrm{BM}}, \qquad \text{[S6]}$$

$$Z_{\mathrm{C}} = \lambda_{\mathrm{C}} - i\omega^{-1}K_{\mathrm{C}}, \qquad \text{[S7]}$$

$$Z_{\mathrm{D}} = \lambda_{\mathrm{D}} - i\omega^{-1}K_{\mathrm{D}}. \qquad \text{[S8]}$$

The forces within the hair bundle depend on its displacement; their effect is to counter viscous damping as well as to influence the resonant frequency of the hair-bundle complex. We may decompose these forces into linear and nonlinear parts:

$$\tilde{F}_{\mathrm{int}} = i\omega Z_{\mathrm{HB}}^{\mathrm{act}}\tilde{X}_{\mathrm{HB}} + \tilde{F}_{\mathrm{int}}^{\mathrm{nonlin}}(\tilde{X}_{\mathrm{HB}}). \qquad \text{[S9]}$$

Here the linear term dominates the dynamics for small displacements ensuing from weak sound stimuli and describes the fully active scenario. The nonlinear term connects the active to the passive case that arises for strong sound stimuli.

At the critical value α_*, the displacements are given by Eq. **3**, which can be rewritten using Eq. **S9** as

$$\begin{aligned} \tilde{X}_{\mathrm{HB}} = &\frac{1}{i\omega(Z_{\mathrm{HB}} - Z_{\mathrm{HB}}^{\mathrm{act}})}\tilde{F}_{\mathrm{int}}^{\mathrm{nonlin}}(\tilde{X}_{\mathrm{HB}}) \\ &+ \frac{Z_{\mathrm{D}} + Z_{\mathrm{C}}}{i\omega(Z_{\mathrm{HB}} - Z_{\mathrm{HB}}^{\mathrm{act}})(Z_{\mathrm{BM}} + Z_{\mathrm{D}} + Z_{\mathrm{C}})}\tilde{F}_{\mathrm{ext}}, \end{aligned} \qquad \text{[S10]}$$

$$\tilde{X}_{\mathrm{BM}} = \frac{1}{i\omega(Z_{\mathrm{BM}} + Z_{\mathrm{D}} + Z_{\mathrm{C}})}\tilde{F}_{\mathrm{ext}}. \qquad \text{[S11]}$$

Resonance in hair-bundle motion occurs at the frequency for which $Z_{\mathrm{HB}} - Z_{\mathrm{HB}}^{\mathrm{act}} = 0$. Active hair-bundle motility makes this situation possible. As discussed in the main text, this resonance condition is independent of the properties of the basilar membrane.

Cochlear Hydrodynamics and Traveling Waves. We now incorporate the description for the micromechanics of the organ of Corti into a model for the whole cochlea. In the simplest form, the cochlea is considered as one-dimensional, exhibiting a slow pressure wave. Combining continuity equations and fluid-momentum

equations, this pressure wave obeys the partial differential equation

$$\rho\partial_t^2 X_{\mathrm{BM}} + \Lambda\partial_t X_{\mathrm{BM}} = \frac{1}{2L^2}\partial_r(h\partial_r p). \qquad \textbf{[S12]}$$

Here ρ denotes the density of liquid in the cochlea, L the length of the cochlea, h the height of the scalae, and p and X_{BM} respectively the pressure across and the displacement of the basilar membrane at position r and time t. The coefficient Λ accounts for friction due to fluid motion. Position is measured in units of the cochlear length, such that $r = 0$ corresponds to the basal and $r = 1$ to the apical end. We apply two boundary conditions. First, $p = p_0$ at $r = 0$: a sound-evoked pressure p_0 acts at the stapes. And second, $p = 0$ at $r = 1$: because the two scalae communicate at the helicotrema, the pressure difference between them vanishes at the apical end of the cochlea.

Considering the Fourier coefficients of angular frequency ω, we obtain

$$-\omega^2\rho\tilde{X}_{\mathrm{BM}} + i\omega\Lambda\tilde{X}_{\mathrm{BM}} = \frac{1}{2L^2}\partial_r(h\partial_r\tilde{p}). \qquad \textbf{[S13]}$$

The basilar-membrane displacement $\tilde{X}_{\mathrm{BM}}$ and pressure $\tilde{p}$ are connected through Eq. **1**, with $\tilde{p} = \tilde{F}_{\mathrm{ext}}/A_{\mathrm{BM}}$. A_{BM} denotes the area of a transverse strip of the basilar membrane that has the width of one cell, about 8 μm; all parameters employed in the two-mass model refer to a transverse segment of the cochlear partition of that width. We solve Eq. **S13** numerically with the shooting method in Mathematica 7 (Wolfram Research).

The height h of the scalae varies from about 1 mm at the base to about 200 μm at the apex. Measurements of the fluid pressure in the basal region indicate, however, that the penetration depth of the wave is significantly smaller (2). In our one-dimensional simulations, we therefore use an effective height of 100 μm.

Concerning the map of characteristic frequencies $f_0(r)$ along the cochlea, we consider the chinchilla's hearing range from a maximal frequency of about 30 kHz at the extreme base to a minimum of about 50 Hz at the extreme apex (3). We assume that the resonant frequency of the basilar membrane cannot cover this whole range and is instead given by

$$f_{\mathrm{BM}}(r) = \sqrt{f_{\mathrm{BM,apex}}^2 + [1 - (f_{\mathrm{BM,apex}})/f_{\max})^2]f_0(r)^2}. \qquad \textbf{[S14]}$$

Here $f_{\max} = 30$ kHz denotes the highest characteristic frequency and $f_{\mathrm{BM,apex}} = 1$ kHz the lowest resonant frequency that the basilar membrane exhibits. f_{BM} coincides with f_0 for high frequencies but deviates for frequencies below f_{L} and approaches $f_{\mathrm{BM,apex}}$ in the apical region of the cochlea (Fig. 3B).

The resonant frequency f_{BM} of the basilar membrane is set by its mass and stiffness according to $f_{\mathrm{BM}} = (2\pi)^{-1}\sqrt{K_{\mathrm{BM}}/m_{\mathrm{BM}}}$. We consider K_{BM} to vary proportional to f_{BM} and m_{BM} to vary inversely: $K_{\mathrm{BM}}(r) = K_{\mathrm{BM}}^{\max} f_{\mathrm{BM}}(r)/f_{\max}$ and $m_{\mathrm{BM}}(r) = K_{\mathrm{BM}}(r)/[2\pi f_{\mathrm{BM}}(r)]^2$, with $K_{\mathrm{BM}}^{\max} = 2\ \mathrm{N{\cdot}m^{-1}}$. The mass m_{TM} of the tectorial membrane is assumed to follow the same spatial variation as the basilar membrane masses, albeit with a smaller value: $m_{\mathrm{TM}} = m_{\mathrm{BM}}/5$. The increase in the basilar-membrane and tectorial-membrane masses from base to apex presumably reflects the increasing size of the organ of Corti towards the apex.

For the variation of the mechanomotility coefficient α along the cochlea, and its dependence on the stimulus frequency f, we make the ansatz

$$\alpha(r,f) = \frac{f_c^4}{f_c^4 + f_0(r)^4} \times \frac{[\delta f(r) f_0]^2}{[f^2 - f_0(r)^2]^2 + [\delta f f_0(r)]^2} \times \alpha_*. \qquad \textbf{[S15]}$$

The first factor accounts for the high-frequency cutoff above which the membrane potential, and thus electromotility, can no longer follow hair-bundle displacement on a cycle-by-cycle basis; we use $f_c = 4$ kHz. To yield the ratchet mechanism at lower frequencies, we choose α to be α_* at the natural frequency. The second factor describes how the response changes when the frequency f of stimulation deviates from the natural frequency f_0; we assume that α is close to α_* as long as both frequencies are similar, but otherwise declines in magnitude. The width of the corresponding curve is determined by the parameter δ, which we set at $\delta = 2$. The mechanomotility coefficient $\alpha(r, f = f_0)$ is shown in Fig. 3A.

The linear part of the active hair-bundle force counters viscous damping and provides a vanishing impedance at the natural frequency. Using Eqs. **1**, **2**, and **S9**, this translates into

$$Z_{\mathrm{HB}} - Z_{\mathrm{HB}}^{\mathrm{act}}|_{f=f_0} = -\frac{Z_{\mathrm{BM}}[(1+\alpha)Z_{\mathrm{D}} + Z_{\mathrm{C}}]}{Z_{\mathrm{BM}} + Z_{\mathrm{C}} + Z_{\mathrm{D}}}\bigg|_{f=f_0}. \qquad \textbf{[S16]}$$

We assume that the imaginary part of Z_{HB} is tuned to the natural frequency f_0 such that the active contribution possesses only a real part corresponding to negative damping, $Z_{\mathrm{HB}}^{\mathrm{act}} \equiv \lambda_{\mathrm{HB}}^{\mathrm{act}}$. Note that in the ratchet mechanism, when $\alpha = \alpha_*$, the right-hand side of Eq. **S16** vanishes, so active hair-bundle forces need to overcome only damping associated with hair-bundle motion.

When α and active hair-bundle forces obey Eqs. **S15** and **S16** and nonlinearities from the hair-bundle forces are ignored, the hair-bundle displacement diverges at resonance. In the actual cochlea, noise as well as nonlinearities supervene and lead to a large but finite displacement. In our simulations, we incorporate this effect by considering values for α and $Z_{\mathrm{HB}}^{\mathrm{act}}$ that deviate by 1% from their ideal values given by Eqs. **S15** and **S16**.

Tuning Curves of Auditory-Nerve Fibers Tuning curves of auditory-nerve fibers are computed by assuming that the hearing threshold corresponds to a root-mean-square deflection of the hair bundles of IHCs by 0.3 nm. These bundles are thought to be coupled by fluid motion to the shearing between the reticular lamina and tectorial membrane, and thus to the displacement of the hair bundles of OHCs. Assuming that the displacement X_{IHB} of the hair bundles of inner hair cells is dependent on friction λ_{IHB} and elasticity K_{IHB}, it couples to the OHCs' bundle motion through the relation

$$\lambda_{\mathrm{IHB}}\partial_t(X_{\mathrm{IHB}} - X_{\mathrm{HB}}) + K_{\mathrm{IHB}}X_{\mathrm{IHB}} = 0. \qquad \textbf{[S17]}$$

Upon Fourier transformation, we obtain

$$\tilde{X}_{\mathrm{IHB}} = \frac{i\omega\lambda_{\mathrm{IHB}}}{i\omega\lambda_{\mathrm{IHB}} + K_{\mathrm{IHB}}}\tilde{X}_{\mathrm{HB}}. \qquad \textbf{[S18]}$$

For high frequencies, viscous coupling is strong and the hair-bundle displacements of IHCs and OHCs coincide. For low frequencies, the coupling decreases and the hair-bundle motion of IHCs remains smaller than that of OHCs. This effect underlies the rising thresholds at low frequencies seen on the left limbs of high-frequency tuning curves (Figure 5) as well as in experimental measurements.

The value of 0 dB SPL is defined by a root-mean-square sound-pressure stimulus of 20 μPa. Because this external pressure is enhanced by the middle ear before acting on the stapes, we assume an increase by a factor of 20 (26 dB) (9).

If they have not been detailed in the text above, the parameters of the two-mass model as well as the one-dimensional descriptions of the cochlea and hair-bundle dynamics of IHCs are given in Table S1.

Electrical Regulation of the OHC Membrane Potential. Deflection X_{HB} of the OHCs hair bundles evokes a change $\delta V \equiv V - V_0$ in the membrane potential from its resting value V_0, which leads to a length change $X_{\mathrm{EE}} = -c\delta V$ (see Eq. **S1** and below) with a

coefficient c of about 20 $\mu m \cdot V^{-1}$ (1). The ratchet mechanism relies on a critical value $\alpha_* = -1 - Z_C/Z_D$ of the ratio $\alpha = -X_{EE}/X_{HB}$ between hair-bundle displacement and cell length change. While its exact value depends on the coupling impedances Z_C and Z_D, the real part of α_* is negative. A typical situation $Z_C = Z_D$ leads to the critical value $\alpha_* = -2$. Here we show how such a value of α_* can emerge within a basic model for the regulation of the OHCs membrane potential. The model relies on voltage-regulated outward K^+ channels (10) that counteract the current through the membrane capacitance, as well as a voltage-regulated inward sodium current (11, 12) that can lead to hyperpolarization upon positive hair-bundle deflection.

The apical surface of an OHC, including the hair bundle, is bathed in endolymph at a potential V_E of about 80 mV (Fig. S2). The basolateral part is surrounded by perilymph at ground potential V_P. The electrical behavior can be represented by a simple circuit described by an equation for current conservation:

$$I_{R_a} = I_{R_b} + I_{C_b}. \qquad \textbf{[S19]}$$

Here I_{R_a} denotes the current through the resistance R_a and I_{R_b} and I_{C_b} denote the currents through R_b and C_b, respectively. We assume that R_a results from the conductivity g_a of the mechanotransduction channels in the hair bundle; the current is mainly carried by K^+ ions (13). The conductance of the basolateral cell membrane stems from voltage-regulated K^+ channels (conductance g_b^K) as well as voltage-regulated Na^+ channels (11, 12) (conductance g_b^{Na}). We obtain

$$g_a(V_E - V) = C_b \partial_t V + g_b^K(V - V_P) - g_b^{Na}(V_{Na} - V) \qquad \textbf{[S20]}$$

in which V_{Na} denotes the Na^+ reversal potential and C_b the cell membrane's capacitance. The potential V_0 inside the cell at vanishing hair-bundle displacement $X_{HB} = 0$ follows as

$$V_0 = \frac{g_a^{(0)} V_E + g_b^{Na(0)} V_{Na} + g_b^{K(0)} V_P}{g_a^{(0)} + g_b^{Na(0)} + g_b^{K(0)}} \qquad \textbf{[S21]}$$

in which the superscript (0) denotes the respective conductances at vanishing hair-bundle displacement.

Hair-bundle displacement X_{HB} changes the conductance g_a of the cell's apical membrane. To linear order we obtain

$$g_a = g_a^{(0)} + \left.\frac{\partial g_a}{\partial X_{HB}}\right|_{(0)} X_{HB}. \qquad \textbf{[S22]}$$

The altered apical conductance evokes a change $\delta V = V - V_0$ in the membrane potential which influences the basal K^+ and Na^+ conductances. The K^+ channels are voltage-regulated at an activation time τ. The dynamics of the change $\delta g_b^K = g_b^K - g_b^{K(0)}$ can be described by

$$\tau \partial_t \delta g_b^K = \left.\frac{\partial g_b^K}{\partial V}\right|_{(0)} \delta V - \delta g_b^K \qquad \textbf{[S23]}$$

which results in

$$\widetilde{\delta g_b^K} = \left.\frac{1}{1 + i\omega\tau} \frac{\partial g_b^K}{\partial V}\right|_{(0)} \widetilde{\delta V} \qquad \textbf{[S24]}$$

for oscillatory stimuli $X_{HB} = \tilde{X}_{HB} e^{i\omega t} + c.c.$ at angular frequency ω. The Na^+ channels are rapidly activated; to linear order their conductance follows as

$$g_b^{Na} = g_b^{Na(0)} + \left.\frac{\partial g_b^{Na}}{\partial V}\right|_{(0)} \delta V. \qquad \textbf{[S25]}$$

Linearization of Eq. **S20** yields

$$\begin{aligned} &\left[i\omega C_b + g_a + g_b^K + g_b^{Na} + \left.\frac{1 - i\omega\tau}{1 + \omega^2\tau^2} \frac{\partial g_b^K}{\partial V}\right|_{(0)} (V - V_P) \right. \\ &\left. - \left.\frac{\partial g_b^{Na}}{\partial V}\right|_{(0)} (V_{Na} - V) \right] \widetilde{\delta V} \\ &= \left.\frac{\partial g_a}{\partial X_{HB}}\right|_{(0)} \tilde{X}_{HB}. \end{aligned} \qquad \textbf{[S26]}$$

The mechanomotility coefficient α follows as $\alpha = c\widetilde{\delta V}/\tilde{X}_{HB}$. From Eq. **S26** we note that delayed voltage-regulated K^+ channels can reduce the effect of the membrane capacitance. A large enough voltage dependence of the inward Na^+ channels can then yield hyperpolarization of the cell upon positive deflection of the hair bundle, as requested for the critical value α_*.

Fig. S3 shows the resulting magnitude and phase of α for typical parameters for apical OHCs (Table S2) in dependence on the frequency of hair-bundle stimulation. The values $\partial g_b^K/\partial V = 1.36\ \mu S \cdot V^{-1}$ and $\partial g_b^{Na}/\partial V = 1.85\ \mu S \cdot V^{-1}$ have been chosen to yield the critical value $\alpha_* = -2$ at the frequency $f_0 = 200$ Hz and lie in the range of measured values (10, 11).

1. Dong X, Ospeck M, Iwasa KH (2002) Piezoelectric reciprocal relationship of the membrane motor in the cochlear outer hair cell. *Biophys J* 82:1254–1259.
2. Olson E (1999) Direct measurement of intra-cochlear pressure waves. *Nature* 402:526–529.
3. Heffner RS, Heffner HE (1991) Behavioral hearing range of the chinchilla. *Hear Res* 5213.
4. Santi PA, Muchow DC (1979) Morphometry of the chinchilla organ of corti and stria vascularis. *J Histochem Cytochem* 27:1539–1542.
5. Prokofjeva LI, Chernyi AG (1986) Quantitative characteristics of the basilar membrane in the mammalian cochlea. *Nauchnye Doki Vyss Shkoly Biol Nauki* 11:44–50.
6. Martin P, Hudspeth AJ, Jülicher F (2001) Comparison of a hair bundle's spontaneous oscillations with its response to mechanical stimulation reveals the underlying active process. *Proc Natl Acad Sci USA* 98:14380–14385.
7. Chan DK, Hudspeth AJ (2005) Mechanical responses of the organ of Corti to acoustic and electrical stimulation in vitro. *Biophys J*89:4382–4395.
8. Ashmore J (2008) Cochlear outer hair cell motility. *Physiol Rev* 88:173–210.
9. Puria S, Peake WT, Rosowski JJ (1997) Sound-pressure measurements in the cochlear vestibule of human-cadaver ears. *J Acoust Soc Am* 101:2754–2770.
10. Mammano F, Ashmore JF (1996) Differential expression of outer hair cell potassium currents in the isolated cochlea of the guinea-pig. *J Physiol* 469:639–646.
11. Witt CM, Hu HY, Brownell WE, Bertrand D (1994) Physiologically silent sodium channels in mammalian outer hair cells. *J Neurophysiol* 72:1037–1040.
12. Zenner HP, Oliver D, Plinkert P, Ruppersberg JP (1997) Sodium current expression during postnatal development of rat outer hair cells. *Pflügers Arch Eur J Physiol* 434:1432–2013.
13. Hudspeth AJ (1989) How the ear's works work. *Nature* 341:397–404.
14. Mistrik P, Mullaley C, Mammano F, Ashmore J (2009) Three-dimensional current flow in a large-scale model of the cochlea and the mechanism of amplification of sound. *J Roy Soc Int*6:279–291.
15. Ricci AJ, Crawford AC, Fettiplace R (2003) Tonotopic variation in the conductance of the hair cell mechanotransducer channel. *Neuron* 40:983– 990.
16. Beurg M, Evans MG, Hackney CM, Fettiplace R (2006) A large-conductance calcium-selective mechanotransducer channel in mammalian cochlear hair cells. *J Neurosci* 26:10992–11000.

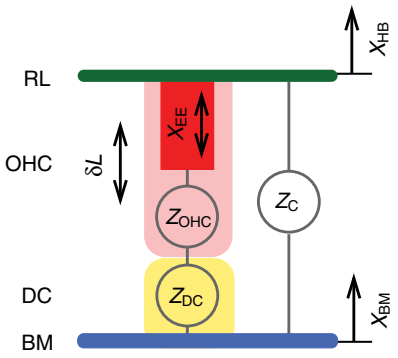

Fig. S1. Coupling between the reticular lamina (RL) and the basilar membrane (BM). The coupling arises from OHCs in series with Deiters' cells (DC) and an impedance Z_C from the remaining organ of Corti. See the text for a description of the coupled OHCs and Deiters' cells.

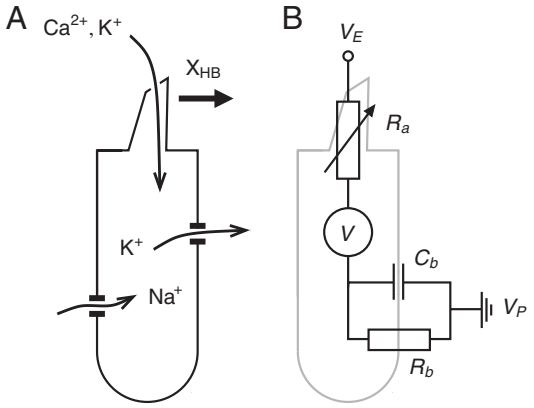

Fig. S2. Regulation of the OHC membrane potential. (*A*) Hair-bundle deflection opens ion channels; K^+ and Ca^{2+} flow into the cell. The cell membrane contains various additional ion channels that are regulated by the membrane potential and the Ca^{2+} concentration. In our model, we consider voltage-regulated outward K^+ channels and inward Na^+ channels. (*B*) An equivalent circuit of an OHC with a variable resistance R_a controlled by hair-bundle displacement, a membrane capacitance C_b, and a basoleteral membrane conductance R_b.

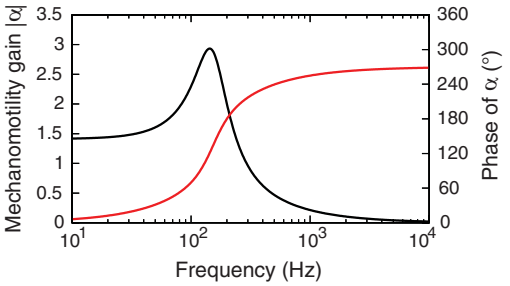

Fig. S3. The modeled mechanomotility coefficient α. We show the dependence of the magnitude (*Black*) and phase (*Red*) of α on the sound frequency. For $f_0 = 200$ Hz the coefficient $\alpha = -2$ emerges, which represents a typical value for the critical α_*. The magnitude of α is strongly attenuated for higher frequencies. By varying the voltage dependence of the basal K^+ and Na^+ channels the critical value α_* can emerge at different frequencies f_0 below a few kilohertz.

Table S1. Parameters used in the cochlear model

Parameter	Description	Value	Reference
L	length of the cochlea	20 mm	[4]
Λ	fluid friction	5×10^5 N · s · m^{-4}	
$w_{BM}(r)$	width of the basilar membrane	(50 + 200r) μm	[5]
$A_{BM}(r)$	area of the basilar-membrane strip	$w_{BM}(r) \times 8$ μm	
λ_{HB}	friction of the hair-bundle complex	1 μN · s · m^{-1}	[6]
K_{IHB}	stiffness of the hair bundles of IHCs	2 mN · m^{-1}	[7]
λ_{IHB}	friction of the hair bundles of IHCs	1 μN · s · m^{-1}	[6]
$\lambda_{BM}(r)$	friction of the basilar membrane	$0.03 \times w_{BM}(r)$ N · s · m^{-2}	
K_C	stiffness of the organ of Corti	10 mN · m^{-1}	
λ_C	friction of the organ of Corti	10 μN · s · m^{-1}	
K_D	stiffness of OHCs and Deiters' cells	20 mN · m^{-1}	[8]
λ_D	friction of OHCs and Deiters' cells	10 μN · s · m^{-1}	

Table S2. Parameters for modeling the regulation of the OHCs membrane potential

Parameter	Description	Value	Reference
V_E	potential of the endolymph	80 mV	[14]
V_P	potential of the perilymph	−100 mV	[14]
V_{Na}	Na^+ reversal potential	22 mV	[11]
$g_a^{K^+}$	apical conductivity of K^+ channels	5 nS	[15]
$g_b^{K^+}$	basolateral K^+ conductivity	10 nS	[10]
C_b	membrane capacitance	40 pF	[10]
$\partial g_a^{K^+}/\partial X_{HB}$	dependence of apical K^+ conductivity on X_{HB}	5 mS · m^{-1}	[16]
τ	activation time of voltage-regulated K^+ channels	1 ms	[10]

Movie S1 Animated illustration of fundamental modes of motion by the organ of Corti. The passive motion is modest, and the hair-bundle movement is similar to that of the basilar membrane. Active hair-bundle motility greatly enhances the motion of both the hair bundles and the basilar membrane. In the ratchet mechanism, only hair-bundle motion is amplified; the basilar membrane moves as in the passive case.

Movie S1 (MOV)